coatings

MDPI

Article

Effect of Glutaraldehyde on Corrosion of X80 Pipeline Steel

Feng Tian [1,2,*] and Lin Pan [2,*]

[1] State Owned Wuhan Xinyu Machine Factory, Wuhan 430060, China
[2] State Key Laboratory of Special Surface Protection Materials and Application Technology, Wuhan Research Institute of Materials Protection, Wuhan 430030, China
* Correspondence: howardtian2004@163.com (F.T.); panlin@rimp.com.cn (L.P.)

Abstract: Glutaraldehyde (GA) is widely employed as a biocide to control microbiologically influenced corrosion in oil fields and industrial water treatment. It might be corrosive to metal. In this study, the effect of glutaraldehyde on the corrosion behavior of X80 pipeline steel was investigated using electrochemical measurement, weight-loss tests and scanning electron microscope (SEM). The weight-loss and electrochemical data show that GA accelerates the corrosion of samples under aerobic conditions, but just slightly influences the corrosion of steel under anaerobic conditions. The results showed that the glutaraldehyde has a minor effect on the corrosion of steel under anaerobic conditions.

Keywords: glutaraldehyde; X80 pipeline steel; biocide; corrosion

Citation: Tian, F.; Pan, L. Effect of Glutaraldehyde on Corrosion of X80 Pipeline Steel. *Coatings* **2021**, *11*, 1176. https://doi.org/10.3390/coatings11101176

Academic Editor: Tadeusz Hryniewicz

Received: 25 August 2021
Accepted: 27 September 2021
Published: 28 September 2021

1. Introduction

Oil production is often carried out by injecting seawater [1–5]. However, the injected seawater often brings nutrients and oxidants, such as sulfates, into the reservoir, so that microorganisms can multiply [6–8]. In the natural environment, microorganisms can cause pipeline corrosion in different industries, including marine environments [9,10], oil fields [11,12] and industrial water systems [13,14]. They can form biofilms on the surface of pipeline steel, metabolize corrosive media, and cause pipeline corrosion, which is called microbiologically influenced corrosion (MIC) [15–17]. MIC accounts for 20% of the total cost of corrosion [18–21].

At present, carbon steel is still used in downhole tubing because of its low cost. Downhole tubing is in an anaerobic environment, so sulfate reducing bacteria (SRB) can multiply in the presence of nutrients and sulfates [22]. Moreover, SRB can obtain electrons from the surface of steel and form sulfide by using sulfate as electron acceptor under anaerobic conditions [23]. SRB can cause corrosion of pipelines [24], and sulfide produced by SRB can lead to oil acidification [3,25]. Therefore, it is essential to inhibit the growth of SRB and protect the pipeline from biological attack. In order to alleviate MIC caused by SRB, biocide treatment is usually needed [26–28]. Because of its broad-spectrum and easy biodegradability, glutaraldehyde is a popular biocide [29,30]. Its terminal aldehyde group can react with amino and sulfhydryl groups of proteins and nucleic acids, thus changing the permeability of cell membranes, which is widely effective against bacteria [31]. Previous studies have shown that glutaraldehyde can inhibit the corrosion of SRB. Wen et al. found [29] that chelators such as EDDS and HEIDA enhanced the inhibitory effect of glutaraldehyde on SRB planktonic cells. Gardner [32] et al. evaluated the effect of antibacterial treatment on sulfate reducing bacteria biofilms and concluded that glutaraldehyde and nitrite can effectively inhibit the formation of sulfide in SRB, and glutaraldehyde treatment is more effective. Xu [30] et al. discovered that the mixed biocide composed of glutaraldehyde, EDDS and methanol had a significant effect on inhibiting the growth of SRB planktonic cells and alleviating corrosion of carbon steel.

There are many studies on glutaraldehyde biocide, but few scholars have studied whether glutaraldehyde is corrosive to pipelines. Therefore, it is important to study whether

glutaraldehyde itself can cause corrosion to the pipeline. In this paper, the influence of different concentrations of glutaraldehyde on the corrosion behavior of X80 pipeline steel was studied using electrochemical measurement methods such as electrochemical impedance spectroscopy (EIS), linear polarization (LP) and potentiometric polarization curve, combined with scanning electron microscopy (SEM), X-ray photoelectron spectroscopy (XPS) and energy dispersive X-ray analysis (EDXA) techniques.

2. Materials and Methods

2.1. Materials and Media

The material used in the experiment is API X80 pipeline steel (Baosteel, Shanghai, China). Its chemical composition (mass percentage, %) is: C 0.07, Mn 1.82, Si 0.19, P 0.007, S 0.023, Cr 0.026, Ni 0.17, Cu 0.02, Al 0.028, Mo 0.23, Ti 0.012, Nb 0.056, V 0.002, N 0.004, B 0.0001, and Fe balance. The electrochemical samples were sealed with epoxy resin, and a working area of 10 mm × 10 mm was reserved. The size of the samples for weight-loss test was 30 mm × 15 mm × 5 mm. All samples were ground with SiC paper, cleaned with deionized water and absolute ethanol, and dried for use. The electrochemical and weight loss samples should be exposed under UV light for at least 20 min before the experiment.

The solution used in the experiment was API-RP 38 medium. The composition of the medium is (g/L): $MgSO_4 \times 7H_2O$ (0.2), NaCl (10), KH_2PO_4 (0.5), ascorbic acid (0.1), sodium lactate (4), yeast extract (1). The pH of the medium was 7.0–7.2. The medium under aerobic conditions was sterilized at 121 °C for 20 min. Under anaerobic conditions, it was deoxygenated by nitrogen for 2 h and sterilized at 121 °C for 20 min.

All anaerobic operations were performed in a clean anaerobic chamber filled with nitrogen. The anaerobic chamber was exposed to UV light for at least 20 min before use.

2.2. Weight Loss Tests

The bottles used for the experiment contained 500 mL medium with 0, 50 or 100 ppm glutaraldehyde. Three replicates were conducted for the weight loss test. Each sample, with a total exposure area of 450 mm^2, was suspended vertically in the medium with a thin wire. After soaking for 1 day, the descaling solution with 500 mL HCl, 500 mL distilled water and 3.5 g hexamethylenetetramine was used to remove the corrosion products on the surface of samples [33]. A fresh descaling solution was used every time and the total cleaning time was less than 2 min. The samples were weighed with an electronic balance before and after the experiment, and the corrosion rate was calculated.

2.3. Scanning Electron Microscopy and X-ray Photoelectron Spectroscopy

After the experiment, a scanning electron microscope (SEM, XL30-FEG, Eindhoven, The Netherlands) was used to observe the morphology of corrosion products on the surface of samples. The elemental composition of corrosion products was obtained by energy dispersive X-ray microanalysis (EDXA, XL30-FEG, Eindhoven, The Netherlands). The chemical valence states of elements were analyzed by X-ray photoelectron spectroscopy (ESCALAB250, Thermo Fisher Scientific, Waltham, MA, USA), and the corrosion products corresponding to binding energy were fitted by XPSPEAK software (version 4.1, Raymund W.M. Kwok, Wise Solutions Inc., Canton, MI, USA).

2.4. Electrochemical Measurements

The PARSTAT 2273 electrochemical workstation (AMETEK, Berwyn, PA, USA) was used to perform electrochemical measurements. The working electrode is X80 pipeline steel. The counter electrode is platinum plate and the reference electrode is a saturated calomel electrode (SCE). The LP curves were measured at a scanning rate of 0.166 mV/s with a scanning range of ±20 mV. Tafel curves were obtained at a scanning rate of 0.166 mV/s within a range of ±250 mV vs. the open circuit potential (OCP). The EIS measurements were recorded with a 10 mV sinusoidal signal in a frequency range of 10^{-2} Hz to 10^5 Hz.

3. Results and Discussion

3.1. SEM Images and Corrosion Products Analysis

Figure 1 shows the SEM images of corrosion products on the surface of samples under aerobic and anaerobic conditions. Compared with anaerobic conditions, there were more corrosion products on the surface of samples under aerobic conditions. Under aerobic conditions, the corrosion products were massive and distributed locally on the surface of samples without the glutaraldehyde. After adding the glutaraldehyde, the corrosion products were layered structures and completely covered the surface of samples. Under anaerobic conditions, no corrosion products were observed for the conditions with the 0 and 50 ppm glutaraldehyde, and only a small amount of corrosion products were found when the concentration of glutaraldehyde increased to 100 ppm.

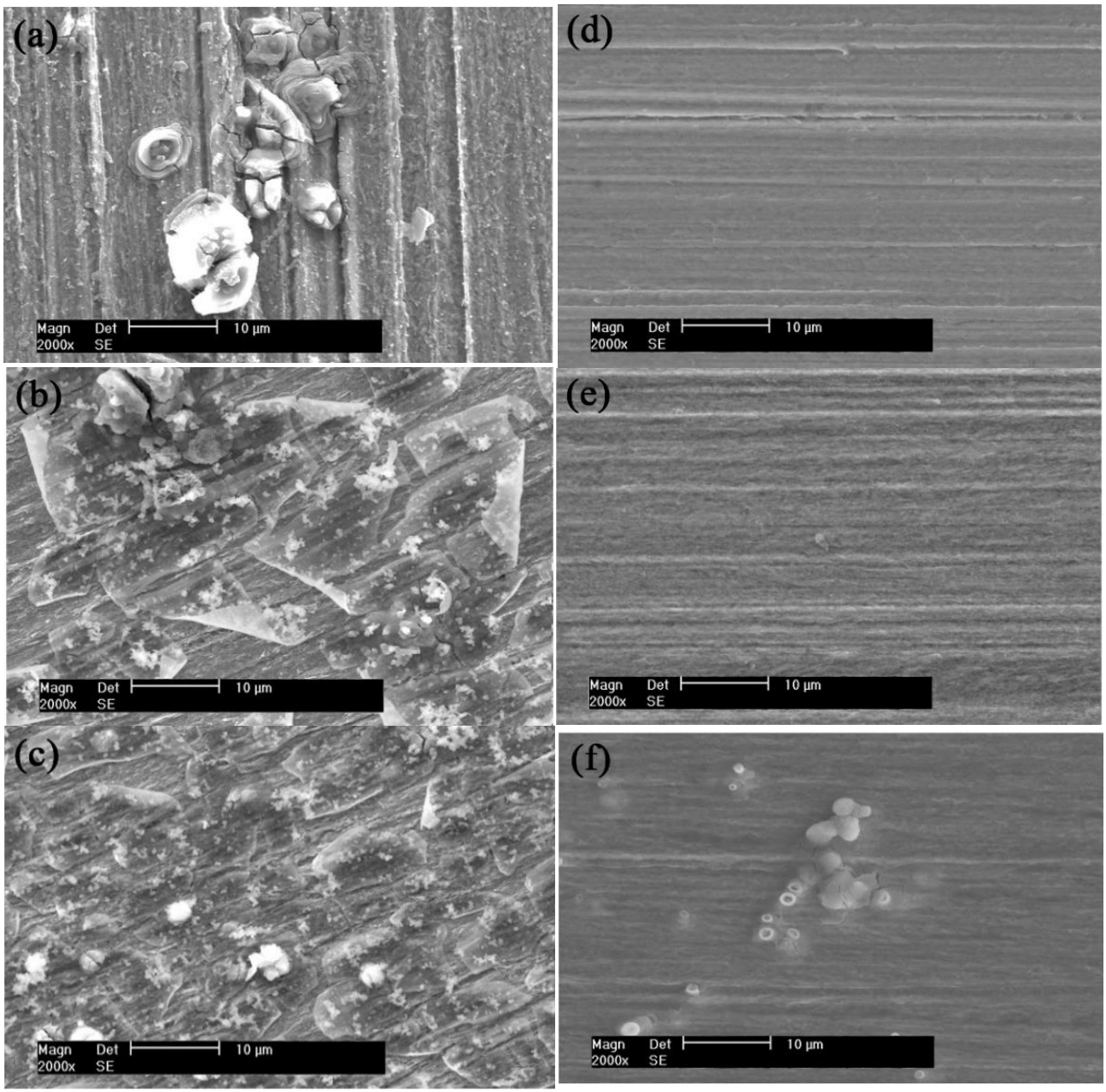

Figure 1. The morphology of corrosion products on the surface of samples under the aerobic conditions with 0 ppm (**a**), 50 ppm (**b**), 100 ppm (**c**) and anaerobic conditions with 0 ppm (**d**), 50 ppm (**e**), 100 ppm (**f**).

The EDXA analysis results of corrosion products are shown in Table 1. The corrosion products under aerobic and anaerobic conditions mainly included elements C, O and Fe. It can be seen from Table 1 that the content of element O was very low for anaerobic conditions with the 0 and 50 ppm glutaraldehyde, which indirectly indicates that there were few corrosion products on the surface of samples. It was consistent with the SEM images in Figure 1d,e.

Table 1. Energy dispersive X-ray (EDXA) results (wt.%) of corrosion products on the surface of samples.

Condition	Concentration (ppm)	Element (%)		
		C	O	Fe
Aerobic conditions	0	9.80	22.20	66.49
	50	8.43	19.26	64.88
	100	9.48	20.55	60.00
Anaerobic conditions	0	6.39	3.13	90.47
	50	4.78	3.33	91.89
	100	7.71	19.65	68.68

X-ray photoelectron spectroscopy was used to further analyze the compositions of corrosion products. Figure 2 shows the high resolution Fe spectrum of corrosion products under aerobic and anaerobic conditions. The corrosion products mainly contain Fe_3O_4, Fe_2O_3 and FeOOH in the conditions with and without the glutaraldehyde.

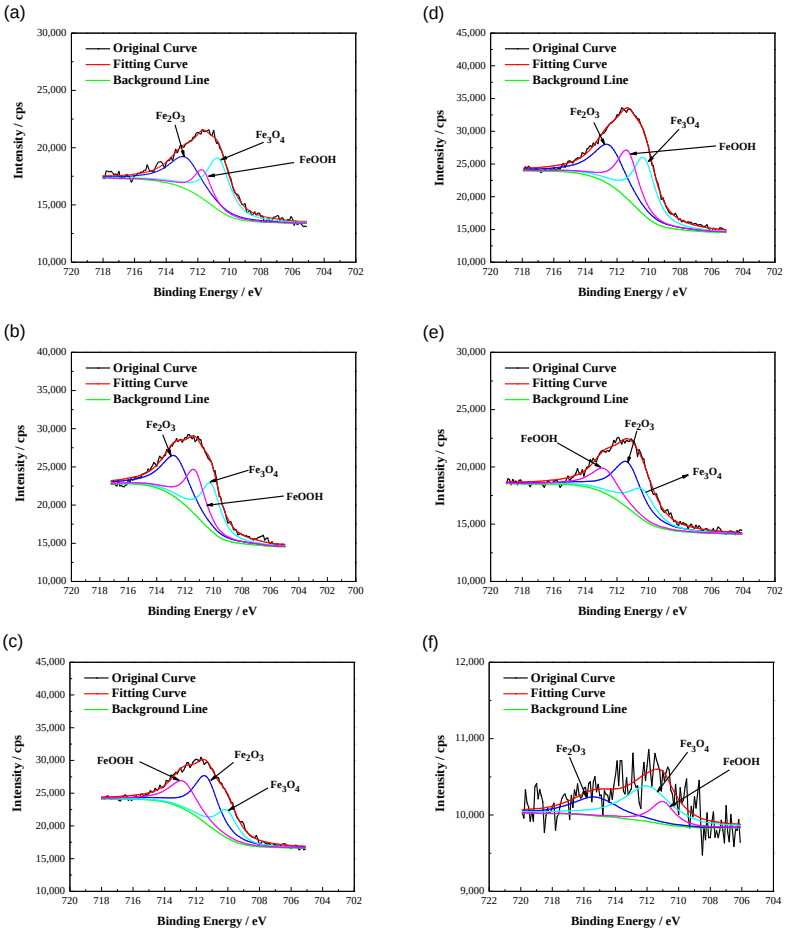

Figure 2. High resolution Fe spectra of corrosion products under the aerobic conditions with 0 ppm (**a**), 50 ppm (**b**), 100 ppm (**c**) and anaerobic conditions with 0 ppm (**d**), 50 ppm (**e**), 100 ppm (**f**).

3.2. Linear Polarization Resistance

Figure 3 shows the change of linear polarization resistance with different concentrations of glutaraldehyde under aerobic and anaerobic conditions. The values of R_P under aerobic conditions are much smaller than those under anaerobic conditions, i.e., the corrosion of steel is much more severe under aerobic conditions than that under anaerobic conditions, which is primarily because oxygen acts as a cathodic depolarizer and can enhance the corrosion of steel. For aerobic conditions, there is a drop of the R_P value when the glutaraldehyde is added, and R_P decreases with the concentration of glutaraldehyde increasing, which indicates that the glutaraldehyde can enhance the corrosion of steel in the presence of oxygen. The SEM images in Figure 1 also confirm it. For anaerobic conditions, there are almost no effects on the corrosion of steel with the addition of glutaraldehyde.

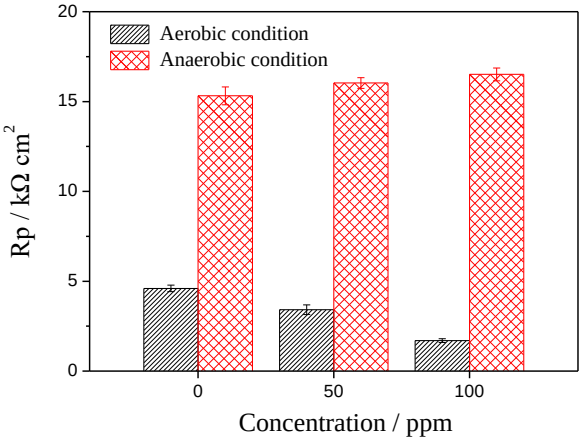

Figure 3. The variation of linear polarization resistance with glutaraldehyde concentration under aerobic and anaerobic conditions.

3.3. Electrochemical Impedance Spectroscopy

The EIS data of different concentrations of glutaraldehyde under aerobic and anaerobic conditions were measured. The Nyquist diagrams are shown in Figure 4. As is well known, there is a negative relationship between the diameter of a capacitive loop and the corrosion rate of a coupon. It can be seen that the diameters of the capacitive loops of samples are much larger under anaerobic conditions than under aerobic conditions, which shows that the corrosion is more severe under aerobic conditions. The diameter of the loop decreases with the increase of glutaraldehyde concentration in the low frequency region.

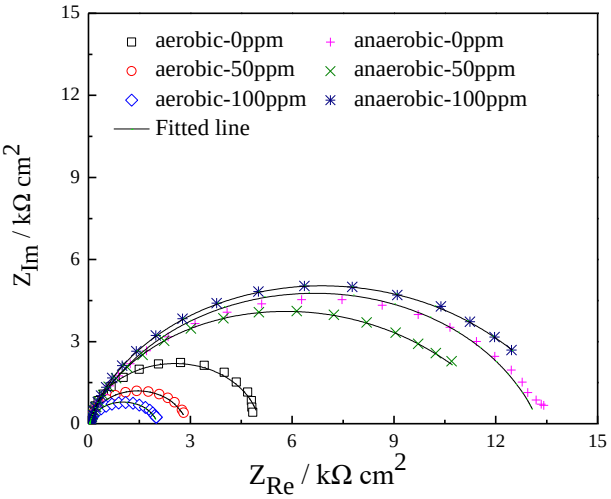

Figure 4. Nyquist diagrams of X80 pipeline steel under aerobic and anaerobic conditions.

The EIS data of different concentrations of glutaraldehyde were analyzed using an equivalent circuit model, shown in Figure 5. The fitting results of EIS measurements are shown in Table 2. R_s represents the solution resistance, and Q_{dl} and R_{ct} represent the double layer capacitance and the charge transfer resistance, respectively. The impedance of constant phase element (CPE) was adopted. As shown below,

$$Z_{CPE} = Y_0^{-1}(j\omega)^{-n} \quad (1)$$

where Y_0 and n are CPE parameters, ω is the angular frequency (rad/s).

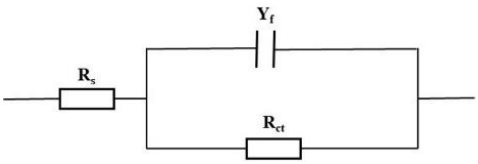

Figure 5. Equivalent circuit model for fitting Nyquist diagrams.

Table 2. Fitting results of electrochemical impedance spectroscopy under aerobic and anaerobic conditions.

Condition	Concentration (ppm)	R_s (Ωcm^2)	$Y_{dl} \times 10^{-4}$ ($Scm^{-2}s^n$)	n_2	R_{ct} ($k\Omega cm^2$)
Aerobic conditions	0	17.95	2.716	0.922	5.030
	50	18.71	3.893	0.893	2.870
	100	15.41	4.811	0.851	2.019
Anaerobic conditions	0	14.38	1.076	0.799	13.27
	50	10.71	1.050	0.894	12.58
	100	16.53	1.107	0.894	14.39

Higher R_{ct} values indicated smaller corrosion rates and stronger corrosion resistance. It can be seen from Table 2 that the R_{ct} values are much larger under anaerobic conditions than under aerobic conditions, which indicates that the reaction at the metal/solution interface is much faster in the presence of oxygen. When the glutaraldehyde is added, the R_{ct} value decreases with the increase of glutaraldehyde under aerobic conditions, which indirectly shows that the glutaraldehyde can further enhance the corrosion of steel under aerobic conditions. The results noted above are consistent with the result of linear polarization resistance.

3.4. Tafel Curves

Figure 6 shows the potentiodynamic polarization curves of samples under aerobic and anaerobic conditions, and the fitting parameters of potentiodynamic polarization curves are given in Table 3. It can be seen that the polarization curves, including anodic and cathodic curves, are almost the same under anaerobic conditions, which indicates that the addition of glutaraldehyde does not affect the reactions of anode and cathode. For aerobic conditions, the polarization curves are different from those in the absence of oxygen, especially for the conditions with glutaraldehyde. With the addition of glutaraldehyde, the anodic curve shifts in the direction of lower current density, which means that the anodic current densities are much smaller than those without glutaraldehyde, as shown in Figure 6a, as the corrosion products formed on the steel surface increase the resistance of the anodic reaction, leading to the decrease in anodic currents. Additionally, it can be found from Table 3 that the Tafel slope of the cathode sharply decreases when the glutaraldehyde is added. It indicates that the glutaraldehyde also changes the cathodic reaction and increases the cathodic current densities (Figure 6a). This result indicates that the addition of glutaraldehyde enhances the corrosion of steel by accelerating the cathodic reaction. The fitting results show that the corrosion current density of steel is 11.72 $\mu A/cm^2$

under aerobic conditions and increases to 14.33 μA/cm^2 with the addition of 100 ppm glutaraldehyde. It can also be seen from Table 3 that the corrosion current densities are much larger under aerobic conditions than under anaerobic conditions.

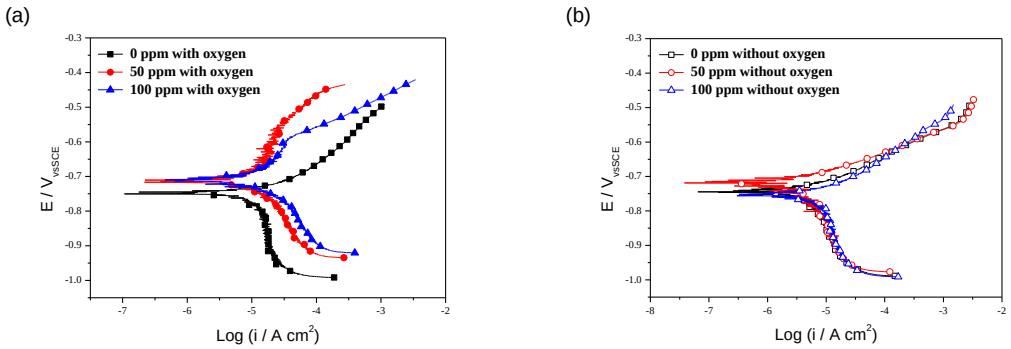

Figure 6. Potentiodynamic polarization curves of samples under aerobic (**a**) and anaerobic (**b**) conditions.

Table 3. Electrochemical parameters fitted by the potentiodynamic polarization curves.

Condition	Concentration (ppm)	E_{corr} (mV)	i_{corr} (μA/cm^2)	β_c (mV·dec^{-1})	β_a (mV·dec^{-1})
Aerobic Conditions	0	−742.9	11.72	468.1	66.1
	50	−687.6	12.48	291.0	159.4
	100	−686.8	14.33	216.0	143.4
Anaerobic Conditions	0	−742.7	5.467	324.6	76.5
	50	−705.2	4.307	280.1	50.0
	100	−739.3	6.565	307.1	60.6

3.5. Weight Loss

After 1 day, the corrosion rates of X80 pipeline steel with different concentrations of glutaraldehyde are shown in Figure 7. The corrosion rates of samples under aerobic conditions were 0.168 mm/year (0 ppm), 0.192 mm/year (50 ppm) and 0.248 mm/year (100 ppm), while those under anaerobic condition were 0.104 mm/year (0 ppm), 0.108 mm/year (50 ppm) and 0.111 mm/year (100 ppm). It can be seen from the data that the glutaraldehyde can promote the corrosion of X80 pipeline steel under aerobic conditions, and the corrosion rate of steel increases with increasing glutaraldehyde concentration. However, the corrosion of glutaraldehyde is very slight under anaerobic conditions. The above results indicate that the glutaraldehyde can be used in the studies of microbiologically influenced corrosion and have few effects on the corrosive behaviors of metals. The weight-loss result is in accordance with the electrochemical results.

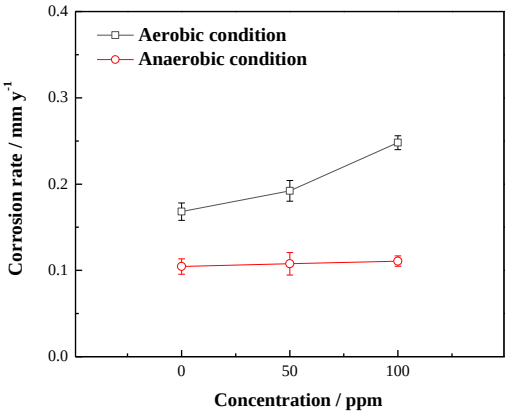

Figure 7. Corrosion rate of X80 pipeline steel with different concentrations of glutaraldehyde under aerobic and anaerobic conditions.

4. Conclusions

In this paper, the effect of glutaraldehyde on the corrosion behavior of X80 steel was studied under aerobic and anaerobic conditions using weight loss tests, electrochemical measurements, and SEM. The conclusions are as follows:

1. The SEM results show that there are corrosion products on the steel surfaces under aerobic conditions, however, almost none under anaerobic conditions. The corrosion products are Fe_3O_4, Fe_2O_3 and FeOOH under both aerobic and anaerobic conditions.
2. The weight-loss and electrochemical results show that the corrosion rates of steel are much larger under aerobic conditions than under anaerobic conditions, and the glutaraldehyde accelerates the corrosion of steel under aerobic conditions, but shows few effects under anaerobic conditions.
3. The formation of corrosion products inhibits the anodic reactions of steel under aerobic conditions, and the glutaraldehyde further enhances the cathodic reaction of steel.
4. There are minor influences of glutaraldehyde on the corrosion of steel under anaerobic conditions.

Author Contributions: F.T.: Conceptualization, Investigation, Data curation, Writing—original draft. L.P.: Review & editing, Supervision. Both authors have read and agreed to the published version of the manuscript.

Funding: This research received no external funding.

Institutional Review Board Statement: Not applicable.

Informed Consent Statement: Not applicable.

Data Availability Statement: Data is contained within the article.

Conflicts of Interest: The authors declare no conflict of interest.

References

1. Veshareh, M.J.; Kjeldsen, K.U.; Findlay, A.J.; Nick, H.M.; Røy, H.; Marietou, A. Nitrite is a more efficient inhibitor of microbial sulfate reduction in oil reservoirs compared to nitrate and perchlorate: A laboratory and field-scale simulation study. *Int. Biodeterior. Biodegrad.* **2021**, *157*, 105154. [CrossRef]
2. Dopffel, N.; Kögler, F.; Hartmann, H.; Costea, P.I.; Mahler, E.; Herold, A.; Alkan, H. Microbial induced mineral precipitations caused by nitrate treatment for souring control during microbial enhanced oil recovery (MEOR). *Int. Biodeterior. Biodegrad.* **2018**, *135*, 71–79. [CrossRef]
3. Shen, Y.; Agrawal, A.; Suri, N.; An, D.; Voordouw, J.; Clark, R.; Jack, T.; Miner, K.; Pederzolli, R.; Benko, A.; et al. Control of microbial sulfide production by limiting sulfate dispersal in a water-injected oil field. *J. Biotechnol.* **2018**, *266*, 14–19. [CrossRef] [PubMed]
4. Zhong, H.; Shi, Z.; Jiang, G.; Yuan, Z. Decreasing microbially influenced metal corrosion using free nitrous acid in a simulated water injection system. *Water Res.* **2020**, *172*, 115470. [CrossRef] [PubMed]
5. Zhong, H.; Shi, Z.; Jiang, G.; Yuan, Z. Synergistic inhibitory effects of free nitrous acid and imidazoline derivative on metal corrosion in a simulated water injection system. *Water Res.* **2020**, *184*, 116122. [CrossRef]
6. Bedoya, K.; Niño, J.; Acero, J.; Cabarcas, F.; Alzate, J.F. Assessment of the microbial community and biocide resistance profile in production and injection waters from an Andean oil reservoir in Colombia. *Int. Biodeterior. Biodegrad.* **2021**, *157*, 105137. [CrossRef]
7. Jia, R.; Yang, D.; Abd Rahman, H.B.; Gu, T. An enhanced oil recovery polymer promoted microbial growth and accelerated microbiologically influenced corrosion against carbon steel. *Corros. Sci.* **2018**, *139*, 301–308. [CrossRef]
8. Unsal, T.; Jia, R.; Kumseranee, S.; Punpruk, S.; Gu, T. Laboratory investigation of microbiologically influenced corrosion of carbon steel in hydrotest using enriched artificial seawater inoculated with an oilfield biofilm consortium. *Eng. Fail. Anal.* **2019**, *100*, 544–555. [CrossRef]
9. Xie, F.; Wang, X.; Wang, D.; Wu, M.; Yu, C.; Sun, D. Effect of strain rate and sulfate reducing bacteria on stress corrosion cracking behaviour of X70 pipeline steel in simulated sea mud solution. *Eng. Fail. Anal.* **2019**, *100*, 245–258. [CrossRef]
10. Lv, M.; Du, M.; Li, X.; Yue, Y.; Chen, X. Mechanism of microbiologically influenced corrosion of X65 steel in seawater containing sulfate-reducing bacteria and iron-oxidizing bacteria. *J. Mater. Res. Technol.* **2019**, *8*, 4066–4078. [CrossRef]

11. Zhou, E.; Wang, J.; Moradi, M.; Li, H.; Xu, D.; Lou, Y.; Luo, J.; Li, L.; Wang, Y.; Yang, Z.; et al. Methanogenic archaea and sulfate reducing bacteria induce severe corrosion of steel pipelines after hydrostatic testing. *J. Mater. Sci. Technol.* **2020**, *48*, 72–83. [CrossRef]
12. Su, H.; Tang, R.; Peng, X.; Gao, A.; Han, Y. Corrosion behavior and mechanism of carbon steel influenced by interior deposit microflora of an in-service pipeline. *Bioelectrochemistry* **2020**, *132*, 107406. [CrossRef]
13. Prithiraj, A.; Otunniyi, I.O.; Osifo, P.; van der Merwe, J. Corrosion behaviour of stainless and carbon steels exposed to sulphate–reducing bacteria from industrial heat exchangers. *Eng. Fail. Anal.* **2019**, *104*, 977–986. [CrossRef]
14. Kokilaramani, S.; Al-Ansari, M.M.; Rajasekar, A.; Al-Khattaf, F.S.; Hussain, A.; Govarthanan, M. Microbial influenced corrosion of processing industry by re-circulating waste water and its control measures-A review. *Chemosphere* **2020**, *265*, 129075. [CrossRef]
15. Arun, D.; Vimala, R.; Ramkumar, K.D. Investigating the microbial-influenced corrosion of UNS S32750 stainless-steel base alloy and weld seams by biofilm-forming marine bacterium Macrococcus equipercicus. *Bioelectrochemistry* **2020**, *135*, 107546. [CrossRef]
16. Parthipan, P.; Sabarinathan, D.; Angaiah, S.; Rajasekar, A. Glycolipid biosurfactant as an eco-friendly microbial inhibitor for the corrosion of carbon steel in vulnerable corrosive bacterial strains. *J. Mol. Liq.* **2018**, *261*, 473–479. [CrossRef]
17. Teng, F.; Guan, Y.; Zhu, W. Effect of biofilm on cast iron pipe corrosion in drinking water distribution system: Corrosion scales characterization and microbial community structure investigation. *Corros. Sci.* **2008**, *50*, 2816–2823. [CrossRef]
18. Cheng, X.; Shi, J.; Wang, W.; Liao, H.; Chen, S.; Liu, G.; Chen, J. Constructing nanostructured functional film on EH40 steel surface for anti-adhesion of Pseudomonas aeruginosa. *Surf. Coatings Technol.* **2021**, *405*, 126683. [CrossRef]
19. Sachan, R.; Singh, A.K. Comparison of microbial influenced corrosion in presence of iron oxidizing bacteria (strains DASEWM1 and DASEWM2). *Constr. Build. Mater.* **2020**, *256*, 119438. [CrossRef]
20. Rasheed, P.A.; Jabbar, K.A.; Rasool, K.; Pandey, R.P.; Sliem, M.H.; Helal, M.; Samara, A.; Abdullah, A.M.; Mahmoud, K.A. Controlling the biocorrosion of sulfate-reducing bacteria (SRB) on carbon steel using ZnO/chitosan nanocomposite as an eco-friendly biocide. *Corros. Sci.* **2019**, *148*, 397–406. [CrossRef]
21. Qian, H.; Zhang, D.; Lou, Y.; Li, Z.; Xu, D.; Du, C.; Li, X. Laboratory investigation of microbiologically influenced corrosion of Q235 carbon steel by halophilic archaea Natronorubrum tibetense. *Corros. Sci.* **2018**, *145*, 151–161. [CrossRef]
22. Vaithiyanathan, S.; Chandrasekaran, K.; Barik, R.C. Green biocide for mitigating sulfate-reducing bacteria influenced microbial corrosion. *3 Biotech* **2018**, *8*, 495. [CrossRef]
23. Dou, W.; Liu, J.; Cai, W.; Wang, D.; Jia, R.; Chen, S.; Gu, T. Electrochemical investigation of increased carbon steel corrosion via extracellular electron transfer by a sulfate reducing bacterium under carbon source starvation. *Corros. Sci.* **2019**, *150*, 258–267. [CrossRef]
24. Parthipan, P.; Elumalai, P.; Narenkumar, J.; Machuca, L.L.; Murugan, K.; Karthikeyan, O.P.; Rajasekar, A. Allium sativum (garlic extract) as a green corrosion inhibitor with biocidal properties for the control of MIC in carbon steel and stainless steel in oilfield environments. *Int. Biodeterior. Biodegrad.* **2018**, *132*, 66–73. [CrossRef]
25. Jurelevicius, D.; Ramos, L.; Abreu, F.; Lins, U.; de Sousa, M.P.; dos Santos, V.V.; Penna, M.; Seldin, L. Long-term souring treatment using nitrate and biocides in high-temperature oil reservoirs. *Fuel* **2021**, *288*, 119731. [CrossRef]
26. Badawi, A.; Hegazy, M.; El-Sawy, A.; Ahmed, H.; Kamel, W. Novel quaternary ammonium hydroxide cationic surfactants as corrosion inhibitors for carbon steel and as biocides for sulfate reducing bacteria (SRB). *Mater. Chem. Phys.* **2010**, *124*, 458–465. [CrossRef]
27. Jia, R.; Yang, D.; Abd Rahman, H.B.; Gu, T. Laboratory testing of enhanced biocide mitigation of an oilfield biofilm and its microbiologically influenced corrosion of carbon steel in the presence of oilfield chemicals. *Int. Biodeterior. Biodegrad.* **2017**, *125*, 116–124. [CrossRef]
28. Struchtemeyer, C.G.; Morrison, M.D.; Elshahed, M.S. A critical assessment of the efficacy of biocides used during the hydraulic fracturing process in shale natural gas wells. *Int. Biodeterior. Biodegrad.* **2012**, *71*, 15–21. [CrossRef]
29. Wen, J.; Zhao, K.; Gu, T.; Raad, I. Chelators enhanced biocide inhibition of planktonic sulfate-reducing bacterial growth. *World J. Microbiol. Biotechnol.* **2009**, *26*, 1053–1057. [CrossRef]
30. Xu, D.; Wen, J.; Gu, T.; Raad, I. Biocide Cocktail Consisting of Glutaraldehyde, Ethylene Diamine Disuccinate (EDDS), and Methanol for the Mitigation of Souring and Biocorrosion. *Corrosion* **2012**, *68*, 994–1002. [CrossRef]
31. Akyon, B.; Lipus, D.; Bibby, K. Glutaraldehyde inhibits biological treatment of organic additives in hydraulic fracturing produced water. *Sci. Total Environ.* **2019**, *666*, 1161–1168. [CrossRef]
32. Gardner, L.R.; Stewart, P.S. Action of glutaraldehyde and nitrite against sulfate-reducing bacterial biofilms. *J. Ind. Microbiol. Biotechnol.* **2002**, *29*, 354–360. [CrossRef]
33. Wei, B.; Qin, Q.; Bai, Y.; Yu, C.; Xu, J.; Sun, C.; Ke, W. Short-period corrosion of X80 pipeline steel induced by AC current in acidic red soil. *Eng. Fail. Anal.* **2019**, *105*, 156–175. [CrossRef]